Phase Behavior of Partially Miscible Ethylene–Styrene Copolymer Blends

ARTICLE *in* MACROMOLECULES · MAY 2001

Impact Factor: 5.8 · DOI: 10.1021/ma002143b

Phase Behavior of Partially Miscible Ethylene−Styrene Copolymer Blends

H. Y. Chen,[†] S. P. Chum,[‡] A. Hiltner,*[,†] and E. Baer[†]

Department of Macromolecular Science and Center for Applied Polymer Research (CAPRI), Case Western Reserve University, Cleveland, Ohio 44106-7202, and Polyolefins and Elastomers R & D, The Dow Chemical Company, Freeport, Texas 77541

Received December 18, 2000

ABSTRACT: Blends of ethylene−styrene copolymers were studied as a model system for miscibility of α-olefin copolymer blends. The phase behavior of partially miscible copolymers, with styrene content difference of 9−10 wt %, was characterized by phase diagrams. Blends were rapidly quenched from the melt to retain the phase morphology, and the volume fractions of the two phases were obtained from AFM phase images. Assuming monodisperse polymers, the phase composition was approximated by extrapolation of the relationship between blend composition and phase volume fraction. The blends exhibited an upper critical solution temperature (UCST). With decreasing molecular weight and decreasing styrene content difference, the blends became more miscible and the UCST decreased. However, the χ interaction parameter extracted from the phase compositions varied with molecular weight, contrary to expectations, and did not show the expected squared dependence on styrene content difference. Much better results were obtained with an approach that considered the molecular weight distribution. Although the polydispersity of ethylene−styrene copolymers is relatively small, the analysis indicated that phase composition depended on initial blend composition. The χ parameter obtained with this approach was independent of molecular weight and was proportional to the square of the styrene content difference. The solubility parameter difference extracted from the χ parameter agreed with literature values.

Introduction

Recent developments in catalyst technology allow for the copolymerization of ethylene with large amounts of styrene.[1] With homogeneous comonomer distribution and narrow molecular weight distribution, these copolymers offer an excellent model system for studying structure−property relationships of ethylene copolymers and miscibility behavior of ethylene copolymer blends.[2−5] A previous study mapped copolymer composition dependence of miscibility and cocrystallization as determined from morphology imaged with atomic force microscopy (AFM), glass transition behavior primarily from dynamic mechanical thermal analysis (DMTA), and melting behavior from differential scanning calorimetry (DSC).[6] A difference in styrene content of about 9 wt % marked a transition from miscible to immiscible ethylene−styrene copolymer blends. The boundary encompassed a very small compositional region, estimated from 9 to 10 wt % styrene content difference, where partial miscibility was clearly evident. In this region, phase behavior was expected to be a strong function of styrene content difference, molecular weight, and temperature. The present study was undertaken to quantify these effects by determining the phase diagram of partially miscible ethylene−styrene copolymer blends.

The typical method of determining a phase diagram is to measure the cloud point of the blend.[7] However, this method is not applicable to blends of ethylene−styrene copolymers due to the chemical similarity of the blend constituents. Alternatively, neutron scattering can be used to probe the phase diagram.[8,9] However, this method requires one constituent to be deuterated. A phase diagram can also be obtained by extrapolating the phase volume fraction to the coexistence phase compositions.[10] As demonstrated in the present study, AFM images are amenable to analysis for phase volume fractions, which are required for this approach.

Most studies that address theoretical and experimental aspects of polymer blend thermodynamics rely on monodisperse species.[11] Because polymer miscibility depends strongly on molecular weight, the effects of molecular weight distribution cannot be neglected with ethylene−styrene copolymers even though their polydispersity is relatively narrow. The consequences of polydispersity were considered theoretically by Solc et al.[12−14] and others[15,16] using an approach based on Flory−Huggins−Staverman thermodynamics and incorporating the molecular weight distribution. Computed phase diagrams for artificial polydisperse blends demonstrated the effects of molecular weight distribution. This approach is now tested against the experimental results for blends of ethylene−styrene copolymers.

Experimental Section

The ethylene−styrene copolymers described in Table 1 were provided by The Dow Chemical Co. The copolymers used in this and previous studies have substantially random incorporation of styrene except that successive head-to-tail styrene chain insertions are shown by ^{13}C NMR analysis to be absent, even with high levels of styrene incorporation. For this reason, the polymers are sometimes described as "pseudorandom" ethylene−styrene interpolymers.[5] The copolymers are designated by the prefix ES, followed by the weight percent styrene. Molecular weight data were provided by Dow. The weight-average molecular weight (M_w) varied from about 120 000 to 250 000 g mol^{-1} with polydispersity less than 2.5. Molecular

[†] Case Western Reserve University.
[‡] The Dow Chemical Company.
* To whom correspondence should be addressed.

10.1021/ma002143b CCC: $20.00
Published on Web 05/03/2001

Table 1. Ethylene−Styrene Copolymers

designation	styrene (wt %)	aPS (wt %)	M_w (kg mol^{-1})	M_w/M_n	T_g (°C) (DMTA, 1 Hz)
ES58(120)	57.6	0.6	120	2.2	10
ES58(168)	57.6	0.8	168	2.1	10
ES58(224)	57.1	0.2	224	1.9	9
ES59(247)	58.8	0.9	247	2.2	12
ES68	67.7	0.5	243	1.8	23

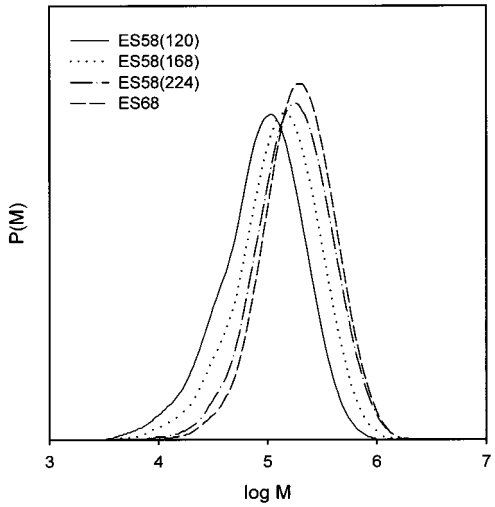

Figure 1. Molecular weight distributions of ES58(120), ES58-(168), ES58(224), and ES68 as weight fraction. The area is normalized to unity.

weight distributions were determined by GPC operating at ambient temperature with THF as the solvent and using polystyrene standards. The data were provided in digital form with 150 equal log M increments. The distributions of ES68 and three copolymers with approximately 58% styrene but differing in molecular weight are shown in Figure 1. For clarity of presentation, the distribution of ES59 is not included in the figure. The glass transition temperature was determined by dynamic mechanical thermal analysis (DMTA) using a DMTA MkII unit from Polymer Laboratories in the tensile mode. The relaxation spectrum was scanned from −50 °C through the glass transition temperature with a frequency of 1 Hz and heating rate of 3 °C min^{-1}.

The copolymers were solution blended. The two constituents were dissolved in refluxing THF for 3−4 h, precipitated with water, and vacuum-dried at ambient temperature. Specimen pans containing approximately 15 mg of the blend were held at the desired temperature in the Rheometrics differential scanning calorimeter (DSC), quenched in dry ice−ethanol mixture to fix the morphology unless otherwise indicated, and removed from the specimen pan. The time at temperature was 1 h for 160 °C and 25 min for temperatures at and above 190 °C. Longer times at temperature produced phase coarsening, but no change in the relative amounts of the two phases, which confirmed that equilibrium phase compositions had been achieved.

Thermal analysis was carried out in a Perkin-Elmer model 7 DSC with approximately 5 mg specimens. The thermograms were obtained with a heating rate of 10 °C min^{-1}. Atomic force microscopy (AFM) was performed on microtomed surfaces with a Digital Instruments Nanoscope IIIa with MultiMode head and J-scanner. The tapping mode was used at ambient conditions. Commercial Si probes were chosen. The resonance frequency of these probes was in the 300 kHz range. Height and phase images were recorded simultaneously. Because of the proximity of the glass transition to ambient temperature, the modulus difference between amorphous copolymers that varied only slightly in styrene content was large enough to provide good contrast in AFM phase images. Image analysis to obtain the area fractions of the two phases was performed by Image-Pro Plus software from Media Cybernetics. The dimension of the square area analyzed varied from 25 to 80 μm depending on the phase size, but was at least 15 times, and sometimes as much as 60 times, the phase dimension. In all cases, two separate areas were analyzed; the analyses differed by less than 3%, and the average is reported.

The copolymers contained a small amount of atactic polystyrene (<1%), which appeared as white spots in the AFM phase images. In addition, all the ES58s and ES59 had a small amount of a rubberlike impurity (<2%) that appeared as black spots in the AFM images. When blending ES58 with ES68, all the atactic polystyrene (aPS) went into the ES68-rich phase and the rubberlike material remained in the ES58-rich phase. Correcting the phase areas for these impurities changed the phase compositions and interaction parameter slightly, however the effect, which was less than 5%, was within the range of experimental uncertainty. Therefore, data were not corrected for these impurities.

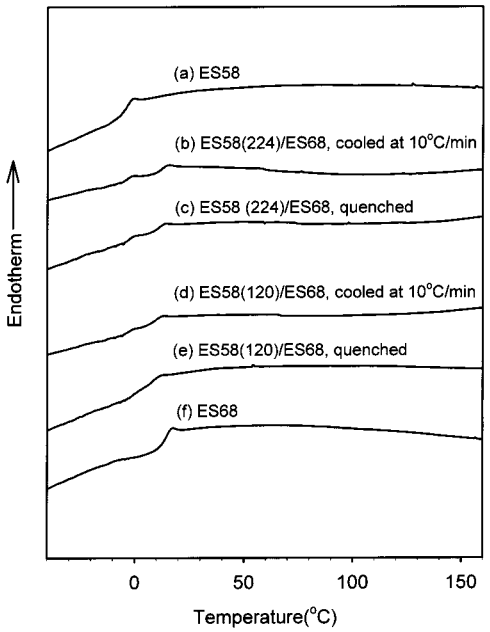

Figure 2. Thermograms of ES58(224)/ES68 and ES58(120)/ES68 (50/50 wt/wt) blends cooled from 190 °C at 10 °C min^{-1} and quenched from 190 °C.

Results and Discussion

Thermal Behavior. The thermal characteristics of partially miscible copolymers were examined in blends of ES68 with ES58(224) of about the same molecular weight and with ES58(120) of lower molecular weight. With 10 wt % difference in styrene content, these blends were expected to form two phases.[6] Indeed, thermograms of the 50/50 wt/wt ES58(224)/ES68 blend that had been slowly cooled from the melt confirmed two glass transitions (T_g's) that were close to the T_g's of the constituents, at −2 °C for ES58 and at 11 °C for ES68 (Figure 2). The DSC thermogram of the slowly cooled 50/50 wt/wt blend of ES68 with the lower molecular weight ES58(120) similarly exhibited two distinct T_g's (Figure 2).

Quenching, instead of cooling slowly, to retain as much as possible the phase condition at 190 °C, did not change the thermal behavior of the ES58(224)/ES68 blend, indicating that phase composition did not noticeably change with temperature. However, if the blend with lower molecular weight ES58(120) was quenched from 190 °C, the two T_g's in the thermogram shifted closer together. This suggested that the blend with lower

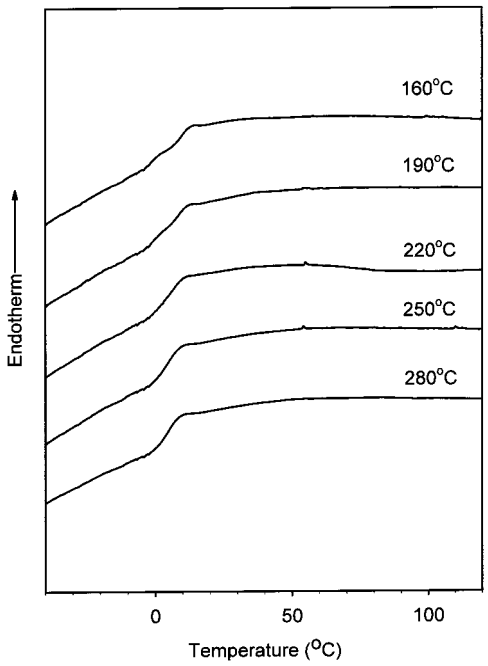

Figure 3. Thermograms of ES58(120)/ES68 (50/50 wt/wt) after quenching from various temperatures.

molecular weight ES58(120) was considerably more miscible at 190 °C than it was at the solidification temperature when slowly cooled, which would have been considerably lower than 190 °C.

The temperature dependence of the phase composition in ES58(120)/ES68 suggested that this blend might have an upper critical solution temperature (UCST). The blend was probed for disappearance of phase separation by quenching to the glassy state from elevated temperatures to fix the melt morphology and subsequently recording the thermogram to obtain the glass transition behavior. A similar approach was previously used to characterize melt miscibility of other blend systems consisting of chemically similar constituents.[17−19] Thermograms of 50/50 wt/wt ES58(120)/ES68 blend quenched from various temperatures are shown in Figure 3. When quenched from the lowest temperature, 160 °C, the blend clearly exhibited two T_g's. As the melt temperature increased, the gradual shift of the T_g's closer together indicated that the blend became more miscible. At 220 °C, two T_g's were almost indistinguishable, and at 250 °C the two T_g's merged into a single sharp glass transition, indicating that the blend formed a single phase. For a blend of two polymers of approximately the same molecular weight, the phase diagram should be symmetrical, and the temperature at which phase separation disappears in the 50/50 blend composition should closely approximate the UCST. The UCST composition of ES58(120)/ES68 would be slightly richer in the lower molecular weight ES58(120) constituent. Therefore, the UCST of ES58(120)/ES68 would be somewhat higher than 250 °C due to the asymmetry of the phase diagram.

Although this technique gives qualitative information about phase behavior, it is difficult to obtain phase composition and therefore the phase diagram. One way to quantify phase composition is to establish a relationship, usually proportionality, between phase composition and glass transition temperature. However, it is hard to precisely identify T_g's from DSC curves. Another approach is to quench the blend from progressively higher temperatures. The lowest temperature at which the quenched blend exhibits a single T_g is taken as the dissolution temperature. This approach has considerable uncertainty; typically changes in temperature of more than 10 °C are needed to produce a noticeable change in glass transition behavior. Therefore, an alternate approach is necessary to determine the coexistence curve.

Phase Behavior with Monodisperse Assumption. Blend composition can be expressed in terms of the phase compositions according to the mass balance relationship

$$\phi_1 = \phi_1' V' + \phi_1'' V'' = (\phi_1' - \phi_1'')V' + \phi_1'' \qquad (1)$$

where ϕ_1 is the overall volume fraction of constituent 1 in the blend, ϕ_1' is the volume fraction of constituent 1 in the constituent 1-rich phase, ϕ_1'' is the volume fraction of constituent 1 in the constituent 2-rich phase, V' is the volume fraction of the constituent 1-rich phase in the blend, and V'' is the volume fraction of the constituent 2-rich phase. If the phase compositions do not depend on the blend composition ϕ_1, as would be the case if the constituents were monodisperse, a plot of ϕ_1 vs V' yields a straight line that extrapolates to the phase compositions ϕ_1' and ϕ_1'' at $V' = 1$ and $V' = 0$.

The phase volume fractions were determined from AFM images of quenched blends. Figure 4 shows the effect of blend composition on the morphology of quenched ES58(120)/ES68 blends. The darker phase is the ES58(120)-rich phase with lower modulus, and the lighter phase is the ES68-rich phase with higher modulus. With increasing ES58(120) content, the ES58(120)-rich phase changed from dispersed to cocontinuous with the ES68-rich phase, to the continuous matrix. The effect of the molecular weight difference was seen by comparing the 40/60 composition (Figure 4a) with the 60/40 composition (Figure 4c): the area of the dispersed ES58(120)-rich phase in 40/60 was considerably smaller than the area of the almost cocontinuous ES68-rich phase in 60/40. This indicated that the lower molecular weight ES58(120) was more soluble in ES68 than vice versa. The primary effect of quench temperature was to change the relative amounts of the two phases. Image analysis was used to determine the phase areas from which the phase volume fractions V' and V'' were calculated.

A typical plot of ϕ_1 vs V' according to eq 1 is shown in Figure 5. The data were approximately described by a linear relationship. With increasing temperature, the slope decreased as the blends became more miscible, and the composition difference between the two phases decreased. Extrapolation gave the coexisting phase compositions for different temperatures (Table 2).

Phase diagrams of ES68 blended with ES58(120) and ES58(168) are compared in Figure 6. It is apparent that both blends became more miscible with increasing temperature, which suggested UCST behavior. However, as the temperature approached the UCST, the composition difference between the phases was small and the sharp contrast between the two phases in AFM images was lost. As a consequence, it was not possible to determine accurately the phase areas. Therefore, the UCST and the phase composition at the UCST were not determined experimentally. The effect of molecular weight was evident in the higher miscibility and the lower apparent UCST of ES58(120)/ES68. A further

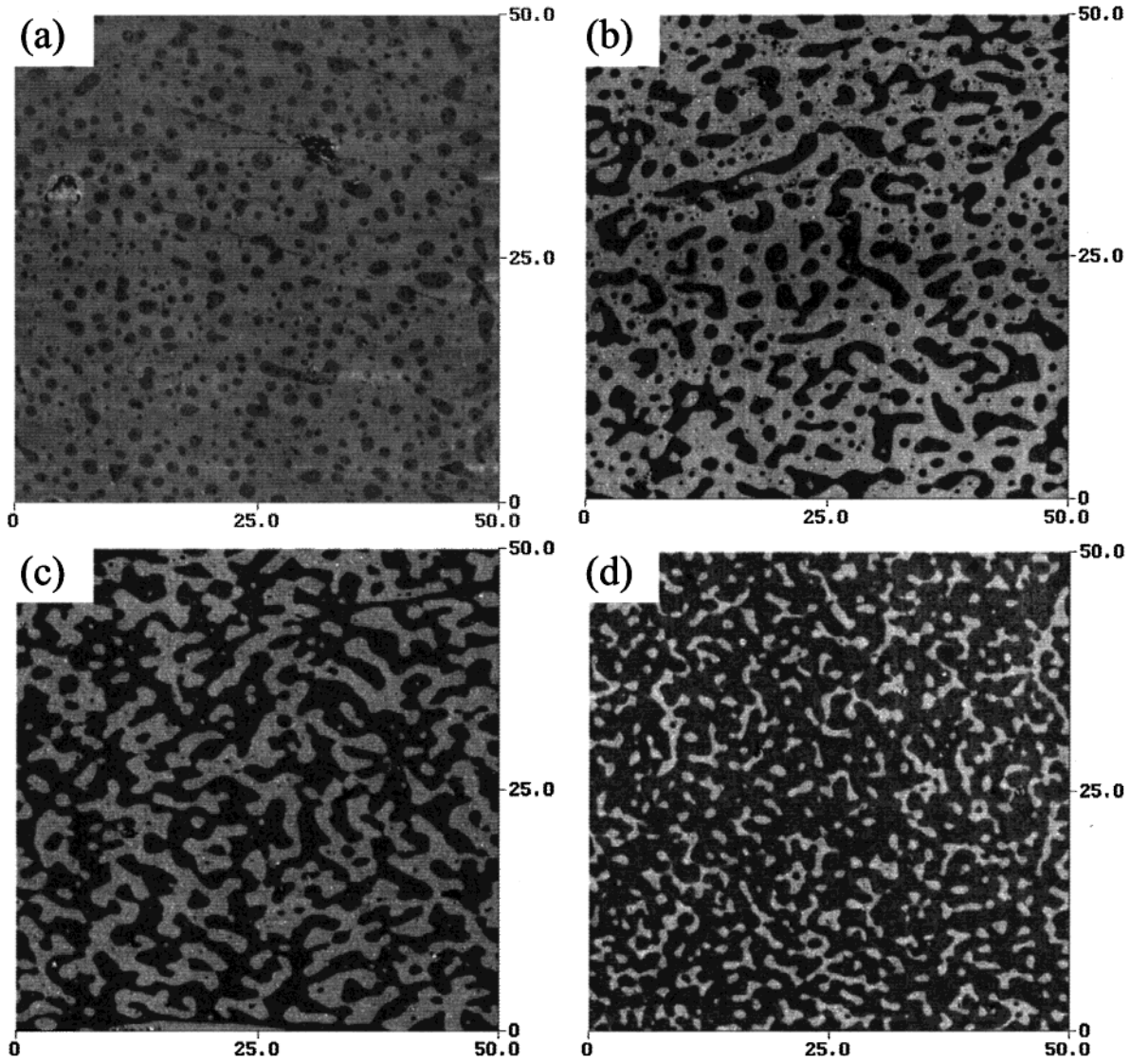

Figure 4. AFM phases images of ES58(120)/ES68 quenched from 190 °C: (a) 40/60 wt/wt, (b) 50/50 wt/wt, (c) 60/40 wt/wt, and (d) 70/30 wt/wt.

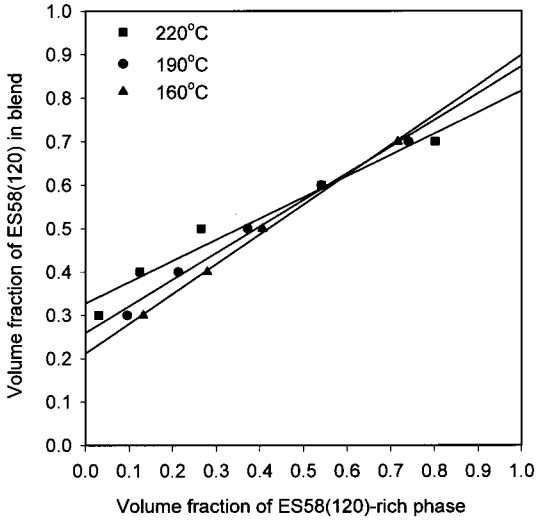

Figure 5. Extrapolation of blend composition vs phase volume fraction to obtain phase compositions of ES58(120)/ES68.

consequence of the molecular weight difference was asymmetry in the phase diagrams of ES58(120)/ES68 and ES58(168)/ES68. Higher solubility of the lower molecular weight constituent caused the asymmetry.

Blends of ES68 with other copolymers of about the same molecular weight demonstrated the effect of copolymer styrene content. With constituents of similar molecular weights, the phase diagrams were symmetrical (Figure 7). The greater miscibility of ES59(247)

Table 2. Phase Compositions and Interaction Parameters Obtained with Assumption of Monodisperse Polymers

	T (°C)	ϕ'_{ES58} or ϕ'_{ES59}	ϕ''_{ES58} or ϕ''_{ES59}	χ assume $M = M_w$
ES58(120)/ES68	160	0.21	0.90	7.4×10^{-4}
	190	0.26	0.87	6.9×10^{-4}
	220	0.33	0.81	6.5×10^{-4}
ES58(168)/ES68	190	0.15	0.91	6.4×10^{-4}
	220	0.20	0.85	5.9×10^{-4}
	250	0.26	0.81	5.5×10^{-4}
	280	0.34	0.77	5.2×10^{-4}
ES58(224)/ES68	190	0.09	0.91	6.0×10^{-4}
	220	0.11	0.90	5.7×10^{-4}
	250	0.15	0.87	5.3×10^{-4}
ES59(247)/ES68	190	0.12	0.86	5.2×10^{-4}
	220	0.16	0.82	4.9×10^{-4}
	250	0.21	0.77	4.6×10^{-4}

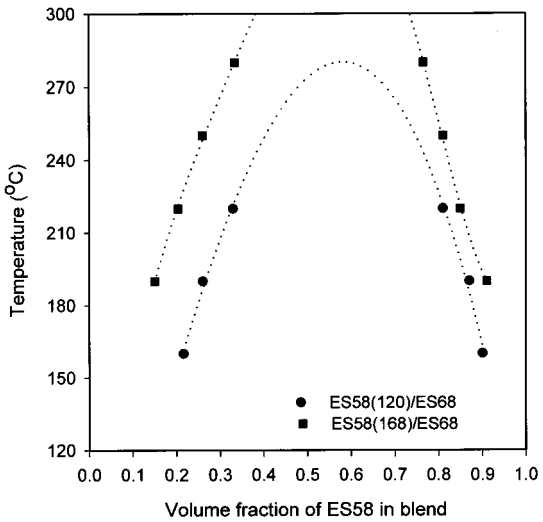

Figure 6. Phase diagrams of ES58(120)/ES68 and ES58(168)/ES68.

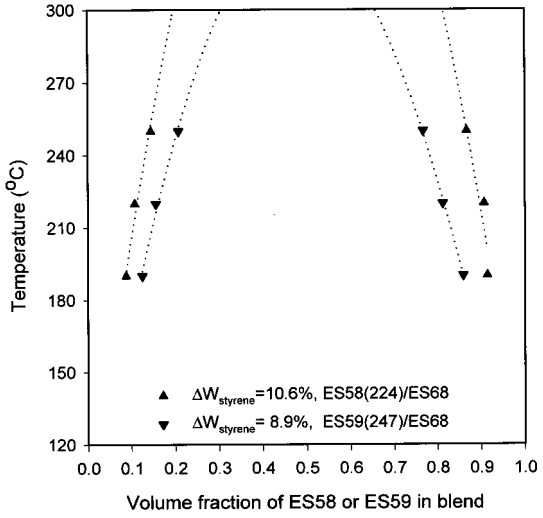

Figure 7. Phase diagrams of ES58(224)/ES68 and ES59(247)/ES68.

compared to that of ES58(224) represented the effect of styrene content difference. With decreasing styrene content difference, the blend became more miscible and the UCST decreased.

The interaction parameter χ can be extracted from the phase diagram by using the Flory−Huggins equation[20]

$$\frac{\Delta G}{RT} = \frac{\phi_1}{N_1 v_1} \ln \phi_1 + \frac{\phi_2}{N_2 v_2} \ln \phi_2 + \frac{\chi}{v} \phi_1 \phi_2 \qquad (2)$$

where N_1 and N_2 are the degrees of polymerization of constituents 1 and 2, v_1 and v_2 are the average molar volumes of the constituent 1 and 2 monomers and are obtained by linear combination based on mole fraction of ethylene (33 mL g^{-1}) and styrene (99 mL g^{-1}), v is the reference volume (taken close to or equal to the smallest of v_1 or v_2, which is assumed to be v_1), and ϕ_1 and ϕ_2 are the volume fractions of constituents 1 and 2 in the blend. In all cases, constituent 1 is identified as the copolymer with the lower styrene content.

With application of the equilibrium condition for equality of constituent chemical potentials in both phases, eq 2 yields

$$\ln \frac{\phi_1'}{\phi_1''} + (\phi_1'' - \phi_1')\left(1 - \frac{N_1 v_1}{N_2 v_2}\right) + \frac{\chi}{v} N_1 v_1 [(1 - \phi_1')^2 - (1 - \phi_1'')^2] = 0 \qquad (3)$$

In this expression, χ is assumed to be independent of blend composition ϕ_1. The weight-average molecular weight was used with eq 3 to calculate χ at each temperature (Table 2). As expected, χ decreased with increasing temperature and decreasing styrene content difference.

The interaction parameter for a blend of ethylene−styrene copolymers conforms to the relationship[21,22]

$$\chi = \chi_{ES}(\psi_1 - \psi_2)^2 \qquad (4)$$

where χ_{ES} is the segmental interaction parameter of ethylene and styrene and ψ_1 and ψ_2 are the volume fractions of styrene in the copolymers.[6] It should be noted that eq 4 appears not to hold for some other α-olefin copolymer blends.[23] This is attributed to an additional contribution to the interaction parameter from local packing effects, which derive from differences in chain flexibility.[24] Equation 4 may work well for ethylene−styrene copolymers because the difference in chain flexibility is negligible for copolymers that differ in styrene content by only 9 wt %. It is apparent from eq 4 that χ decreases with decreasing styrene content difference, and the blend becomes more miscible.

The usual temperature dependence of χ suggests that χ_{ES} decreases as the temperature is raised according to the relationship[25]

$$\chi_{ES} = a + \frac{b}{T} \qquad (5)$$

For ethylene−styrene copolymers, the volume fraction is approximately equal to weight fraction, and the latter was used to plot $\chi_{ES} = \chi(\psi_1 - \psi_2)^{-2}$ vs T^{-1} in Figure 8. The data scattered about a linear regression with $a = -0.024$ and $b = 40$ (K). Although χ was not expected to depend on molecular weight of the blend constituents, the results of the monodisperse analysis presented in Table 2 and plotted in Figure 8 demonstrated a systematic decrease in χ with decreasing molecular weight of the ES58 constituent.

The critical values of interaction parameter χ_c and composition ϕ_c at the UCST are given by the Flory−Huggins analysis as

$$\chi_c = \frac{1}{2}\left(\frac{1}{\sqrt{N_1}} + \frac{1}{\sqrt{N_2(v_2/v_1)}}\right)^2 \qquad (6)$$

$$\phi_c = \frac{\sqrt{N_2(v_2/v_1)}}{\sqrt{N_1} + \sqrt{N_2(v_2/v_1)}} \qquad (7)$$

Extrapolation of the temperature dependence of χ to χ_c gave the UCST of ES58(120)/ES68 as 274 °C and the UCST of ES58(164)/ES68 as 307 °C. The critical composition at the UCST from eq 7 was 0.58 for ES58(120)/ES68 and 0.54 for ES58(164)/ES68. The critical composition should be about 0.50 if the two constituents have similar molecular weights, as with ES58(224)/ES68 and ES59(247)/ES68 blends.

Phase Behavior Considering Molecular Weight Distribution. The demonstrated strong molecular

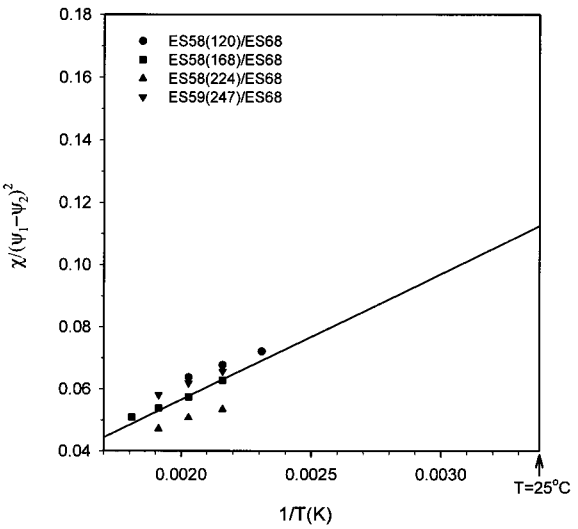

Figure 8. Reduced χ parameter from monodisperse analysis vs reciprocal temperature for all blends.

weight dependence of miscibility, and the systematic molecular weight variation in χ obtained from the monodisperse analysis of blends with the same styrene content difference, indicate that the molecular weight distribution cannot be neglected in phase diagram construction of ethylene−styrene copolymer blends even though the molecular weight distribution is relatively narrow. Low molecular weight fractions of one constituent are always more miscible with the other constituent than the high molecular weight fractions. Therefore, at equilibrium, both phases consist of high molecular weight fractions of one constituent and low molecular weight fractions of the other constituent. In other words, the molecular weight distribution of a constituent is not the same in both phases and is not the same as the original distribution. Moreover, the molecular weight distributions should change with blend composition. As a consequence, phase composition depends on blend composition, and the linear extrapolation of eq 1 becomes invalid.

The thermodynamic approach developed by Solc and co-workers incorporates the molecular weight distribution of the blend constituents.[12] In the general case of two polydisperse constituents identified by the subscripts 1 and 2, the free energy of mixing for a blend of composition ϕ_2 is given by

$$\frac{\Delta G}{RT} = \sum_i n_{1i} \ln \phi_{1i} + \sum_j n_{2j} \ln \phi_{2j} + \chi\phi_2 \sum_i n_{1i} r_{1i} \qquad (8)$$

where n is moles of chains and ϕ is volume fraction in the blend of the monodisperse fractions identified by the subscripts i and j for constituents 1 and 2, respectively. The relative chain length r is defined as the number of basic units in a chain, and the volume fraction of such chains in the blend is $\phi_{1i} = n_{1i}r_{1i}/r_{\text{total}}$ and $\phi_{2j} = n_{2j}r_{2j}/r_{\text{total}}$ where $r_{\text{total}} = \sum n_{1i}r_{1i} + \sum n_{2j}r_{2j}$. Using the average monomer of constituent 1 as the basic unit, $r_{1i} = N_{1i}$ and $r_{2j} = N_{2j}(v_2/v_1)$, where N is the degree of polymerization and v_1 and v_2 are the average monomer volumes of constitutents 1 and 2, respectively.

At equilibrium, the chemical potential of each fraction is the same in both phases. Thus, the calculation of equilibrium concentrations involves the solution for a system of equations. However, the number of equations can be reduced dramatically by introducing two separation factors, σ_1 and σ_2, where the partitioning of each fraction between the two phases (indicated by $'$ and $''$) obeys the relation[20]

$$\sigma_1 = r_{1i}^{-1}(\ln \phi''_{1i} - \ln \phi'_{1i}) \qquad (9a)$$

and

$$\sigma_2 = r_{2j}^{-1}(\ln \phi''_{2j} - \ln \phi'_{2j}) \qquad (9b)$$

for all i and j. Therefore, the system of equilibrium equations is reduced to two equations

$$\sigma_1(\phi'_1 + \phi''_1) + \sigma_2(\phi'_2 + \phi''_2) - 2\left[\left(\frac{\phi''_1}{r''_{n1}} + \frac{\phi''_2}{r''_{n2}}\right) - \left(\frac{\phi'_1}{r'_{n1}} + \frac{\phi'_2}{r'_{n2}}\right)\right] = 0 \qquad (10)$$

and

$$\sigma_2 - \sigma_1 = 2\chi(\phi''_1 - \phi'_1) \qquad (11)$$

where r'_{n1}, r''_{n1}, r'_{n2} and r''_{n2} are the number-average chain lengths of each constituent in each phase

$$r'_{n1} = \phi'_1\left(\sum_i \frac{\phi'_{1i}}{r_{1i}}\right)^{-1}, \text{ etc.} \qquad (12)$$

Additional mass balance equations are used to compute the phase compositions and χ. Volume additivity upon demixing gives

$$\phi'_{1i} + R_v\phi''_{1i} = (R_v + 1)\phi_{1i} = (R_v + 1)\phi_1 W_{1i} \qquad (13a)$$

and

$$\phi'_{2j} + R_v\phi''_{2j} = (R_v + 1)\phi_{2j} = (R_v + 1)\phi_2 W_{2j} \qquad (13b)$$

where $R_v = V''/V'$ is the volume ratio of the two phases, ϕ_1 and ϕ_2 are the volume fractions of constituents 1 and 2 in the blend, and W_{1i} and W_{2j} are the weights of fractions i and j in constituents 1 and 2, respectively. Combining eq 13 with eq 9, the definition of the separation factor, gives

$$\phi'_1 = \sum_i \phi'_{1i} = (R_v + 1)\phi_1 \sum_i \frac{W_{1i}}{1 + R_v \exp(\sigma_1 r_{1i})} \qquad (14a)$$

and

$$\phi'_2 = \sum_j \phi'_{2j} = (R_v + 1)\phi_2 \sum_j \frac{W_{2j}}{1 + R_v \exp(\sigma_2 r_{2j})} \qquad (14b)$$

Finally, combining eq 14 with the mass balance expression $\phi_1 + \phi_2 = \phi'_1 + \phi'_2$ gives

$$\phi_1 \sum_i \frac{W_{1i}}{1 + R_v \exp(\sigma_1 r_{1i})} + \phi_2 \sum_j \frac{W_{2j}}{1 + R_v \exp(\sigma_2 r_{2j})} - \frac{1}{1 + R_v} = 0 \qquad (15)$$

Equations 10 and 15 are solved simultaneously to obtain

Table 3. Phase Compositions and Interaction Parameters Obtained by Considering Molecular Weight Distribution

		$\phi_{ES58} = 0.3$ or $\phi_{ES59} = 0.3$			$\phi_{ES58} = 0.4$ or $\phi_{ES59} = 0.4$			$\phi_{ES58} = 0.7$ or $\phi_{ES59} = 0.7$			average
	T (°C)	ϕ'_{ES58} or ϕ'_{ES59}	ϕ''_{ES58} or ϕ''_{ES59}	χ (10^{-4})	ϕ'_{ES58} or ϕ'_{ES59}	ϕ''_{ES58} or ϕ''_{ES59}	χ (10^{-4})	ϕ'_{ES58} or ϕ'_{ES59}	ϕ''_{ES58} or ϕ''_{ES59}	χ (10^{-4})	χ (10^{-4})
ES58(120)/ES68	160	0.22	0.83	8.2	0.22	0.86	9.2	0.34	0.84	8.1	8.5 ± 0.7
	190	0.25	0.80	7.4	0.29	0.78	7.7	0.37	0.82	7.5	7.5 ± 0.2
	220	0.28	0.75	6.6	0.35	0.74	6.6	0.46	0.76	6.5	6.6 ± 0.1
ES58(168)/ES68	190	0.17	0.84	7.8	0.16	0.87	8.2	0.29	0.84	6.9	7.6 ± 0.7
	220	0.21	0.80	6.7	0.22	0.82	7.2	0.32	0.81	6.3	6.7 ± 0.5
	250	0.25	0.75	5.9	0.28	0.76	6.1	0.35	0.79	6.0	6.0 ± 0.1
	280	0.28	0.69	5.3	0.39	0.64	5.0	0.42	0.74	5.3	5.1 ± 0.2
ES58(224)/ES68	190	0.08	0.92	10.0	0.13	0.86	7.9	0.14	0.90	8.5	8.8 ± 1.2
	220	0.13	0.84	7.4	0.17	0.82	6.8	0.18	0.88	7.3	7.2 ± 0.4
	250	0.15	0.82	6.8	0.18	0.81	6.6	0.23	0.83	6.2	6.5 ± 0.3
ES59(247)/ES68	190	0.15	0.81	6.7				0.20	0.85	6.4	6.6 ± 0.2
	220	0.18	0.77	5.7				0.26	0.81	5.5	5.6 ± 0.1
	250	0.23	0.71	5.0				0.32	0.76	4.8	4.9 ± 0.1

σ_1 and σ_2. A unique solution is obtained in the case of polydisperse constituents because phase composition and phase volume ratio depend on blend composition. However, for monodisperse constituents, phase composition is independent of blend composition, and eqs 10 and 15 are degenerate. Consequently, at least two sets of data (phase volume ratio and blend composition) are needed to obtain phase composition of blends with monodisperse constituents.

The quantities W_{1i} and W_{2j} were taken from the molecular weight distributions in Figure 1. The 150 molecular weight fractions provided for each constituent were reduced to 15 fractions of equal log M intervals to decrease the calculation time. Although phase compositions and number-average chain lengths were not known, they could be written as functions of σ_1 and σ_2. The Mathematica software was used to solve eqs 10 and 15. Subsequently, eqs 11 and 14 were used to calculate χ and the phase compositions ϕ'_1 and ϕ''_1. Because the calculation for blend compositions close to the critical value was very sensitive to experimental uncertainty, only data for $\phi_{ES58} = 0.3$, 0.4, and 0.7 and $\phi_{ES59} = 0.3$ and 0.7 were analyzed.

The results in Table 3 were consistent with χ independent of blend composition. Although the values of χ scattered, they did not exhibit a systematic change with blend composition. Conversely, phase compositions depended on blend composition. This was most evident if the constituent molecular weights were different, so that one of the constituents was more soluble than the other. Thus, there was a large and systematic increase in concentration of the lower molecular weight ES58(120) or ES58(168) in the ES58-poor phase as the ES58 concentration in the blend increased. However, the composition of the other phase (i.e., the concentration of the higher molecular weight ES68 in the ES68-poor phase) did not change significantly over the blend compositions studied.

The dependence of phase composition on blend composition is more apparent in the molecular weight distribution of the constituents in each phase. The phase compositions ϕ'_{1i} and ϕ''_{1i} for a given fraction with r_{1i}, and likewise ϕ'_{2j} and ϕ''_{2j} for r_{2j}, were calculated from eqs 9 and 13. The calculation was performed for each of the 150 molecular weight fractions provided. Figure 9 shows the distributions of ES58(120) and ES68 in each phase for blend compositions ϕ_1 of 0.3 and 0.7 at 220 °C. The peaks in Figure 9 are normalized so that the areas are proportional to the phase composition. Comparison of the molecular weight distribution of either constituent in the constituent-rich phase with the distribution in the constituent-poor phase demonstrates the preferential dissolution of the lower molecular weight fractions.

The higher solubility of ES58(120) in ES68 than vice versa is evident by comparing the peak areas of the minor constituent (ES58 in the ES58-poor phase and ES68 in the ES58-rich phase) at either blend composition. Furthermore, the increase in ES58 fraction in the ES58-poor phase (ϕ'_{ES58}) as the blend becomes richer in ES58 is evident by comparing the area under the ES58 distribution at the two blend compositions (compare ES58 distributions in Figure 9a,c). The dependence of phase composition on blend composition is a direct consequence of constituent polydispersity: as ES58 becomes the major constituent, there is more of the low molecular weight ES58 available to dissolve in less ES68. The concentration of ES58 in the ES58-rich phase (ϕ''_{ES58}) should also increase as ϕ_1 increases from 0.3 to 0.7. (This is equivalent to an increase in ES68 in the ES68-poor phase as the blend becomes richer in ES68.) Assuming χ to be independent of composition, the incremental change in composition of the ES58-rich phase is much smaller than the change in the ES58-poor phase. The estimated change is 0.02 for an increase in ϕ_1 from 0.3 to 0.7, which is within the uncertainty of the Table 3 calculations. However, the change in molecular weight distribution of ES68 in the ES58-rich phase as it becomes the major phase is evident (compare ES68 distributions in Figure 9b,d).

The same calculation is presented for blends with constituents of comparable molecular weight in Figure 10. In contrast to the ES58(120) distribution in the previous example, the ES58(224) fraction in the ES58-poor phase increases only slightly as the blend composition changes (compare parts a and c of Figure 10). Moreover, because both constituents have similar molecular weights, the amount of minor constituent is similar in the ES58-rich and ES58-poor phases, consistent with the symmetrical phase diagram. Indeed, if the constituents have identical molecular weight and molecular weight distribution, they are interchangeable, and the distributions in the 0.3 and 0.7 blends will mirror each other. The ES58(224)/ES68 blend closely approximates this situation. However, even if the molecular weight distributions are identical, because the constituents are polydisperse, the phase compositions will change with blend composition. If χ is independent of blend composition, the incremental change in phase composition for a change in ϕ_1 from 0.3 to 0.7 is about 0.05, which is close to the observed changes in Table 3.

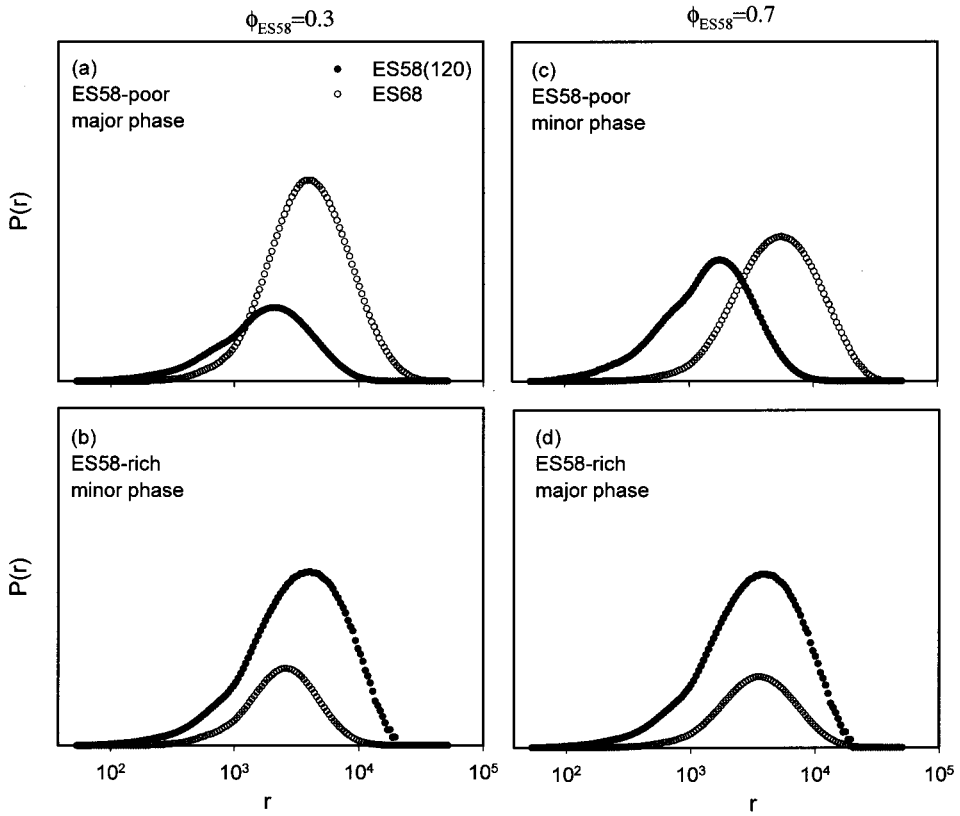

Figure 9. Molecular weight distributions of ES58(120) and ES68 in both phases for blend compositions ϕ_1 of 0.3 (a, b) and 0.7 (c, d) at 220 °C.

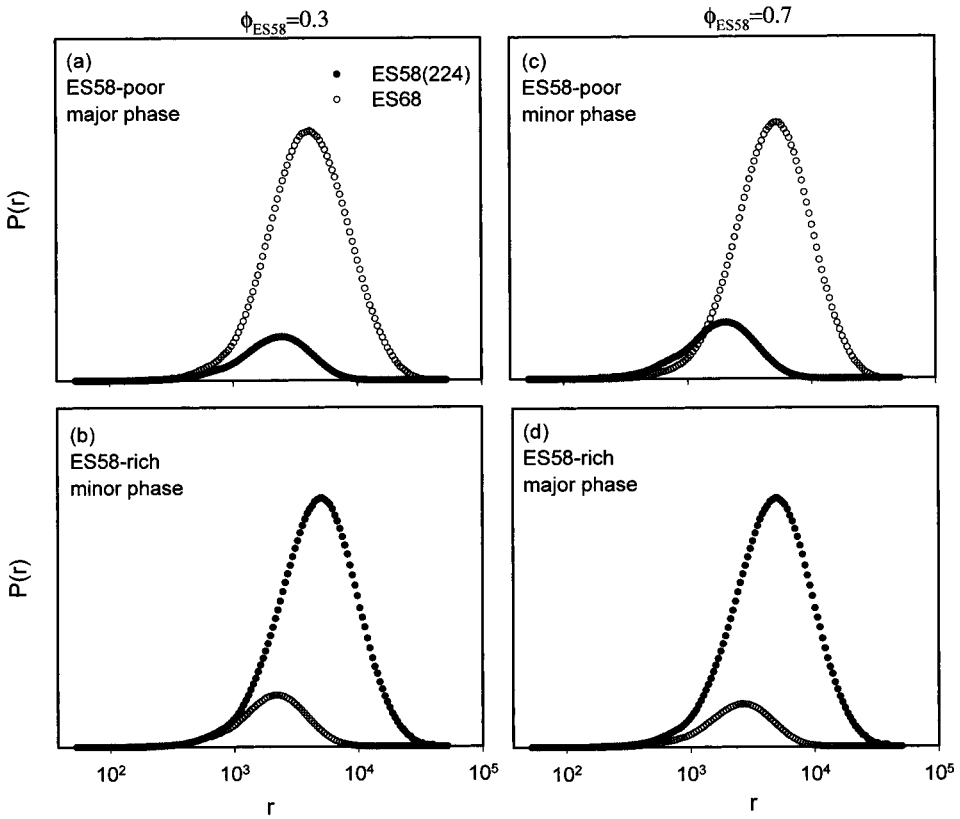

Figure 10. Molecular weight distributions of ES58(224) and ES68 in both phases for blend compositions ϕ_1 of 0.3 (a, b) and 0.7 (c, d) at 220 °C.

The dependence of phase composition on blend composition suggests that the linear extrapolation according to eq 1 is only an approximation. The data from Figure 5 are plotted again in Figure 11 where they are compared with the relationship between blend composition and volume fraction of the ES58(120)-rich phase

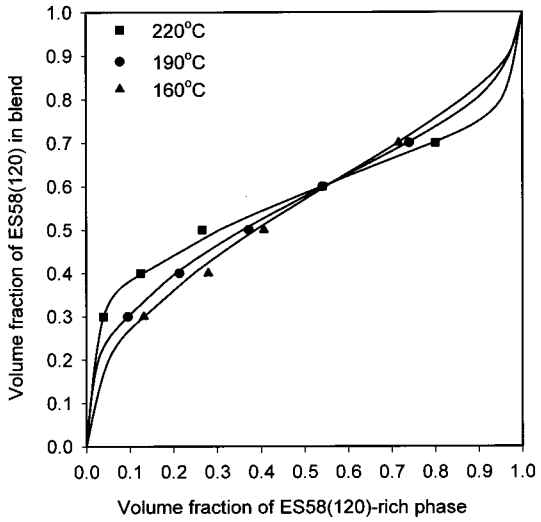

Figure 11. Relationship between blend composition and volume fraction of the ES58(120)-rich phase for ES58(120)/ES68. Symbols are experimental data. Lines are calculated from polydisperse analysis assuming χ to be independent of composition.

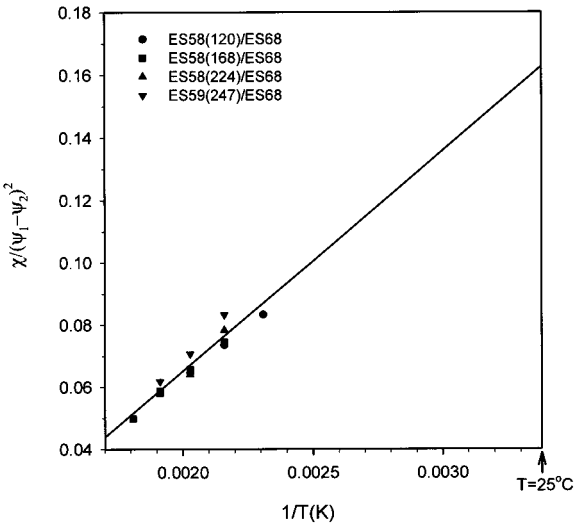

Figure 12. Reduced χ interaction parameter from polydisperse analysis vs reciprocal temperature for all blends.

calculated for the ES58(120)/ES68 blend, assuming χ to be independent of blend composition. The calculation was performed following the procedure used to obtain χ from the experimental R_v values. For each blend composition, the volume fraction of the ES58(120)-rich phase (R_v) was varied until the value of χ matched the χ value in Table 3 at the composition $\phi_1 = 0.3$. It is evident that the polydisperse analysis describes the data better. A linear correlation is possible if compositional extremes are avoided. Particularly if the constituents have similar molecular weights, phase compositions of ethylene−styrene copolymer blends do not experience large changes with blend composition. Then, phase compositions obtained by extrapolation are useful for constructing an approximate phase diagram. However, comparison of the two approaches clearly demonstrates that χ cannot be reliably extracted from the monodisperse approximation. For any blend of polydisperse constituents, extraction of χ using eq 2 is unreliable because the system cannot be represented by a single degree of polymerization for each constituent, N_1 and N_2.

The temperature dependence of χ is plotted in Figure 12 as $\chi(\psi_1 - \psi_2)^{-2}$ vs T^{-1} in accordance with eqs 4 and 5. A linear relationship satisfactorily accommodated all the data from the polydisperse analysis, in contrast to the results of the monodisperse approximation (Figure 8). The linear regression gave $a = -0.076$ and $b = 71$ (K). The parameter a is usually found to be positive in accordance with identification of a as an entropic contribution.[26] However, in at least one instance, similar values of $a = -0.101$ and $b = 81$ (K) were reported for blends of linear polyethylene with atactic polybutene.[11]

The average χ values were comparable to those obtained with the monodisperse assumption using weight-average molecular weight. In terms of χ, the monodisperse and polydisperse analyses gave numerically similar results for copolymers with relatively narrow molecular weight distribution in the temperature range examined. However, the monodisperse assumption predicted a much weaker temperature dependence with $a = -0.024$ and $b = 40$ (K). This would have led to significant errors for any extrapolation, for example, to ambient temperature.

Extrapolation of the temperature dependence from the polydisperse analysis gave $\chi_{ES} = 0.162$ at 25 °C. This can be compared with the estimation from solubility parameters

$$\chi_{ES} = \frac{V_{ref}}{RT}(\delta_{PE} - \delta_{PS})^2 \qquad (16)$$

where δ_{PE} and δ_{PS} are the solubility parameters of the ethylene and styrene homopolymers; $V_{ref} = (V_E V_S)^{1/2}$ is the reference volume with $V_E = 33$ cm^3 mol^{-1} for the ethylene unit and $V_S = 99$ cm^3 mol^{-1} for the styrene unit. From eq 16, $\delta_{PE} - \delta_{PS}$ was calculated to be 2.6 (MPa)$^{1/2}$, which is consistent with literature values, which are in the range 2.0−3.3 (MPa)$^{1/2}$.[27] This discussion considers the constituents as random copolymers of ethylene and styrene, whereas they are more accurately described as random copolymers of ethylene and ethylene−styrene diads.[5] Indeed, the absence of head-to-tail styrene substitution significantly affects properties that depend on chain flexibility such as glass transition temperature and plateau modulus.[4] The interaction parameter, on the contrary, is predominantly an enthalpic term. As such, it depends on average composition and should not be as sensitive as chain dynamics to systematic nonrandomness on the scale of a few repeat units.

Summary

In summary, blends of ethylene−styrene copolymers were used as a model system for studying the miscibility of α-olefin copolymer blends. The coexistence window, from 9 to 10 wt % difference in styrene content, where blends demonstrated partial miscibility with an upper critical solution temperature, was exploited to examine the consequences of molecular weight, molecular weight distribution, and styrene content difference. Conventional methods for imaging domain morphology were inappropriate for partially miscible blends because of the similarity in chemical composition of the constituents. However the modulus differences were large enough that AFM phase images clearly revealed the domain morphology. Although the copolymers had

relatively narrow molecular weight distributions with M_w/M_n of about 2, analysis of the data assuming monodispersity gave unsatisfactory results. This provided an opportunity to test the approach of Solc and co-workers, based on the Flory−Huggins−Staverman equation, which incorporates polydispersity. The interaction parameter extracted from this approach was independent of molecular weight and demonstrated the expected squared dependence on styrene content difference of the constituents. Utilizing the known molecular weight distributions, subsequent calculations revealed the extent to which the phase compositions depended on the initial blend composition.

Acknowledgment. The authors thank Dr. Martin J. Guest and Dr. Y. Wilson Cheung of The Dow Chemical Co. for providing technical assistance. The financial support of The Dow Chemical Co. is gratefully acknowledged.

References and Notes

(1) The Dow Chemical Company, U.S. Patent 5,703,187; E.P. Patent 416,815A1.
(2) Chen, H. Y.; Stepanov, E. V.; Chum, S. P.; Hiltner, A.; Baer, E. *J. Polym. Sci., Part B: Polym. Phys.* **1999**, *37*, 2373−2382.
(3) Chen, H. Y.; Stepanov, E. V.; Chum, S. P.; Hiltner, A.; Baer, E. *Macromolecules* **1999**, *32*, 7587−7593.
(4) Chen, H. Y.; Stepanov, E. V.; Chum, S. P.; Hiltner, A.; Baer, E. *Macromolecules* **2000**, *33*, 8870−8877.
(5) Chen, H. Y.; Guest, M. J.; Chum, S. P.; Hiltner, A.; Baer, E. *J. Appl. Polym. Sci.* **1998**, *70*, 109−119.
(6) Chen, H. Y.; Cheung, Y. W.; Hiltner, A.; Baer, E. *Polymer*, in press.
(7) Nishi, T.; Kwei, T. K. *Polymer* **1975**, *16*, 285−290.
(8) Reichart, G. C.; Graessley, W. W.; Register, R. A.; Lohse, D. J. *Macromolecules* **1998**, *31*, 7886−7894.
(9) Alamo, R. G.; Londono, J. D.; Mandelkern, L.; Stehling, F. C.; Wignall, G. D. *Macromolecules* **1994**, *27*, 411−417.
(10) Pellegrini, N. N.; Winey, K. I. *Macromolecules* **2000**, *33*, 73−79.
(11) Balsara, N. P.; Fetters, L. J.; Hadjichristidis, N.; Lohse, D. J.; Han, C. C.; Graessley, W. W.; Krishnamoorti, R. *Macromolecules* **1992**, *25*, 6137−6147.
(12) Solc, K.; Koningsveld, R. *Collect. Czech. Chem. Commun.* **1995**, *60*, 1689−1718.
(13) Koningsveld, R.; Solc, K. *Collect. Czech. Chem. Commun.* **1993**, *58*, 2305−2320.
(14) Vanhee, S.; Koningsveld, R.; Berghmans, H.; Solc, K.; Stockmayer, W. H. *Macromolecules* **2000**, *33*, 3924−3931.
(15) Clarke, N.; McLeish, T. C. B.; Jenkins, S. D. *Macromolecules* **1995**, *28*, 4650−4659.
(16) Mumby, S. J.; Sher, P. *Macromolecules* **1994**, *27*, 689−694.
(17) Ueda, H.; Karasz, F. E. *Macromolecules* **1985**, *18*, 2719−2723.
(18) Lehr, M H. *Polym. Eng. Sci.* **1985**, *25*, 1056−1068.
(19) Crist, B.; Hill, M. J. *J Polym. Sci., Part B: Polym. Phys.* **1997**, *35*, 2329−2353.
(20) Flory, P. J. *Principles of Polymer Chemistry*, Cornell University Press: Ithaca, NY, 1953; Chapter 13.
(21) Scott, R. L. *J. Polym. Sci.* **1952**, *9*, 423−432.
(22) ten Brinke, G.; Karasz, F. E.; MacKnight, W. J. *Macromolecules* **1983**, *16*, 1827−1832.
(23) Graessley, W. W.; Krishnamoortic, R.; Balsara, N. P.; Butera, R. J.; Fetters, L. J.; Lohse, D. J.; Schulz, D. N. *Macromolecules* **1994**, *27*, 3896−3901.
(24) Fredrickson, G. H.; Liu, A. J.; Bates, F. S. *Macromolecules* **1994**, *27*, 2503−2511.
(25) Utracki, L. A. *Polymer Alloys and Blends*; Hanser: Munich, 1989; Chapter 2.
(26) Freed, K. F.; Dudowicz, J. *Macromolecules* **1996**, *29*, 625−636.
(27) Brandrup, J.; Immergut, E. H. In *Polymer Handbook*, 3rd ed.; Wiley-Interscience: New York, 1989; Chapter 7.

MA002143B